Reward prediction error does not explain movement selectivity in DMS-projecting dopamine neurons

Rachel S. Lee, Marcelo G. Mattar, Nathan F. Parker, Ilana B. Witten, Nathaniel D. Daw

Princeton Neuroscience Institute
Department of Psychology
Princeton University, Princeton, NJ, USA 08550

Abstract:

Although midbrain dopamine (DA) neurons have been thought to primarily encode reward prediction error (RPE), recent studies have also found movement-related DAergic signals. For example, we recently reported that DA neurons in mice projecting to dorsomedial striatum are modulated by choices contralateral to the recording side. Here, we introduce, and ultimately reject, a candidate resolution for the puzzling RPE vs movement dichotomy, by showing how seemingly movement-related activity might be explained by an action-specific RPE. By considering both choice and RPE on a trial-by-trial basis, we find that DA signals are modulated by contralateral choice in a manner that is distinct from RPE, implying that choice encoding is better explained by movement direction. This fundamental separation between RPE and movement encoding may help shed light on the diversity of functions and dysfunctions of the DA system.

Introduction

A central feature of dopamine (DA) is its association with two apparently distinct functions: reward and movement (Niv et al. 2007; Berke 2018). Although manipulation of DA produces gross effects on movement initiation and invigoration, physiological recordings of DA neurons have historically shown few neural correlates of motor events (Wise 2004; Schultz, Dayan, and Montague 1997). Instead, classic studies reported responses to rewards and reward-predicting cues, with a pattern suggesting that DA neurons carry a "reward prediction error" (RPE) – the difference between expected reward and observed reward – for learning to anticipate rewards (Schultz, Dayan, and Montague 1997; Andrew G. Barto 1995; Cohen et al. 2012; Coddington and Dudman 2018; Soares, Atallah, and Paton 2016; Hart et al. 2014). In this classic framework, rather than explicitly encoding movement, DA neurons influence movements indirectly, by determining which movements are learned, and/or the general motivation to engage in a movement (Niv et al. 2007; Collins and Frank 2014; Berke 2018).

Complicating this classic view, however, several recent studies have suggested that subpopulations of DA neurons may have a more direct role in encoding movement (Parker et al. 2016). For example, we recently reported that whereas dopamine neurons projecting to ventral striatum showed classic RPE signals, a subset of midbrain DA neurons that project to the dorsomedial striatum (DMS) were selective for a mouse's choice of action (Parker et al. 2016). In particular, they responded more strongly during contralateral (versus ipsilateral) choices as mice perform a probabilistic learning task (Parker et al. 2016). In addition, there have been several other recent studies that reported phasic changes in DA activity at the onset of spontaneous movements (Dodson et al. 2016; Howe and Dombeck 2016; da Silva et al. 2018; Barter et al. 2015; Syed et al. 2016). In addition, other studies have shown that DA neurons may also have other forms of apparently non-RPE signals, such as signals related to novel or aversive stimuli (Menegas et al. 2017; Horvitz 2000; Ungless, Magill, and Bolam 2004; Matsumoto and Hikosaka 2009; Lammel et al. 2011).

These recent observations of movement selectivity leave open an important question: can the putatively movement-related signals be reconciled with Reinforcement Learning (RL) models describing the classic RPE signal? For instance, while it seems plausible that movement-related DA signals could influence movement via directly modulating striatal medium spiny neurons (DeLong 1990), these signals are accompanied in the same recordings by RPEs which are thought to drive corticostriatal plasticity (Reynolds, Hyland, and Wickens 2001). It is unclear how these two qualitatively different messages could be teased apart by the recipient neurons. Here we introduce and test one possible answer to this question, which we argue is left open by Parker et al.'s (2016) results and also by other reports of movement-related DA activity: that these movement-related signals actually also reflect RPEs, but for reward predictions tied to particular movement direction. Specifically, computational models like the actor-critic (A. G. Barto, Sutton, and Anderson 1983) and advantage learning (Baird 1994) learn separate

predictions about the overall value of situations or stimuli and about the value of specific actions. It has long been suggested these two calculations might be localized to ventral vs dorsal striatum, respectively (Montague, Dayan, and Sejnowski 1996; O'Doherty et al. 2004; Takahashi, Schoenbaum, and Niv 2008). Furthermore, a human neuroimaging experiment reported evidence of distinct prediction errors for right and left movements in the corresponding contralateral striatum (Gershman, Pesaran, and Daw 2009).

This leads to the specific hypothesis that putative movement-related signals in DMS-projecting DA neurons might actually reflect an RPE related to the predicted value of contralateral choices. If so, this would unify two seemingly distinct messages observed in DA activity. Importantly, a choice-specific RPE could explain choice-related correlates observed prior to the time of reward. This is because temporal difference RPEs do not just signal error when a reward is received, they also have a phasic anticipatory component triggered by predictive cues indicating the availability and timing of future reward, such as (in choice tasks) the presentation of levers or choice targets (Montague, Dayan, and Sejnowski 1996; Morris et al. 2006; Roesch, Calu, and Schoenbaum 2007). This anticipatory prediction error is proportional to the value of the future expected reward following a given choice – indeed, we henceforth refer to this component of the RPE as a "value" signal, which tracks the reward expected for a choice. Crucially, a choice-specific value signal can masquerade as a choice signal because, by definition, action and value are closely related to each other: animals are more likely to choose actions they predict have high value. In this case, a value signal (RPE) for the contralateral choice will tend to be larger when that action is chosen than when it is not (Samuelson 1938). Altogether, given the fundamental correlation between actions and predicted value, a careful examination of the neural representation of both quantities, and a clear understanding of if and how they can be differentiated, is required to determine whether or not movement direction signals can be better explained as value-related.

Thus, we examined whether dopamine signals in DMS-projecting DA neurons are better understood as a contralateral movement signal or as a contralateral RPE. To tease apart these two possibilities, we measured neural correlates of value and lateralized movement in our DA recordings from mice performing a probabilistic learning task. Since value predictions are subjective, we estimated value in two ways: 1) by using reward on the previous trial as a simple, theory-neutral proxy, and 2) by fitting the behavioral data with a more elaborate trial-by-trial Q-learning model. We compared the observed DA modulations to predictions based on modulation either by movement direction, and/or the expected value (anticipatory RPE) of contralateral or chosen actions.

Ultimately, our results show that DMS-projecting DA neurons' signals are indeed modulated by value (RPE), but, crucially, this modulation reflected the value of the chosen action rather than the contralateral one. Thus, the value aspects of the signals (which were not lateralized) could not explain the contralateral choice selectivity in these neurons, implying that this choice-dependent modulation indeed reflects modulation by contralateral movements and not value.

Results

Task, behavior and DA recordings

Mice were trained on a probabilistic reversal learning task as reported previously (Parker et al. 2016). Each trial began with an illumination in the nose port, which cued the mouse to initiate a nose poke (**Figure 1a**). After a 0-1s delay, two levers appeared on both sides of the nose port. Each lever led to reward either with high probability (70%) or low probability (10%), with the identity of the high probability lever swapping after a block of variable length (see Methods for more details, **Figure 1b**). After another 0-1s delay, the mouse either received a sucrose reward and an accompanying auditory stimulus (positive conditioned stimulus, or CS+), or no reward and a different auditory stimulus (negative conditioned stimulus, or CS-).

Given that block transitions were not signaled to the mouse, after each transition mice gradually learned to prefer the lever with the higher chance of reward. To capture this learning, we fitted their choices using a standard trial-by-trial *Q*-learning model that predicted the probability of the animal's choice at each trial of the task (**Figure 1c, Table 1**). In the model, these choices were driven by a pair of decision variables (known as Q-values) putatively reflecting the animal's valuation of each option.

As mice performed this task, we recorded activity from either the terminals or cell bodies of DA neurons that project to DMS (VTA/SN::DMS) using fiber photometry to measure the fluorescence of the calcium indicator GCaMP6f (**Figure 1d,e; Figure 1-Figure Supplement 1a,b**). As previously reported, this revealed elevated activity during contralateral choice trials relative to ipsilateral choice trials, particularly in relation to the nose poke and lever presentation events (**Figure 1f,g; Figure 1-Figure Supplement 1c**) (Parker et al. 2016).

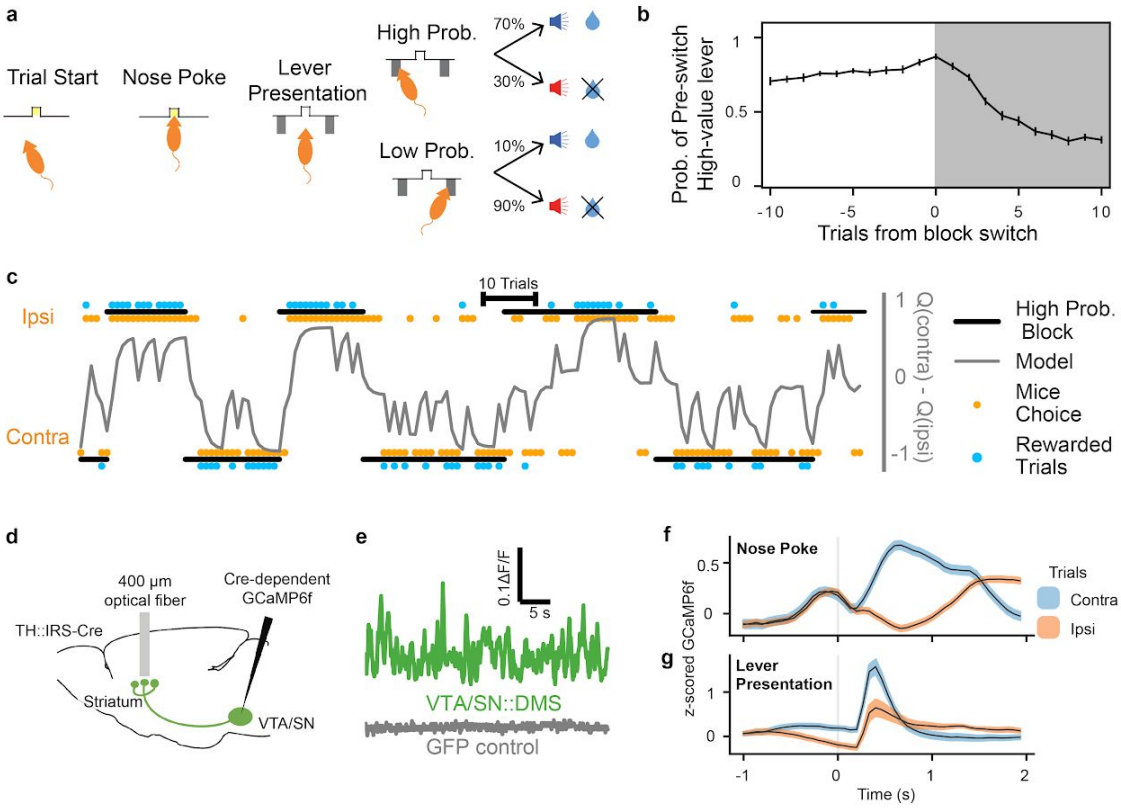

Figure 1: Mice performed a probabilistic reversal learning task during GCaMP6f recordings from VTA-SN::DMS terminals or cell bodies. (**a**) Schematic of a mouse performing the task. The illumination of the central nosepoke signaled the start of the trial, allowing the mouse to enter the nose port. After a 0-1 second jitter delay, two levers are presented to the mouse, one of which results in a reward with high probability (70%) and the other with a low probability (10%). The levers swapped probabilities on a pseudorandom schedule, unsignaled to the mouse. (**b**) The averaged probability of how likely the mice were to choose the lever with high value before the switch, 10 trials before and after the block switch, when the identity of the high value lever reversed. Error bars indicate +/- 1 standard error (n = 19 recording sites). “Contra” and “Ipsi” refer to the location of the lever relative to the side of the recording. (**c**) We fitted behavior with a trial-by-trial Q learning mixed effect model. Example trace of 150 trials of a mouse's behavior compared to the model’s results. Black bars above and below the plot indicate which lever had the high probability for reward; Orange dots indicate the mouse’s actual choice; Blue dots indicate whether or not mouse was rewarded; Grey line indicate the difference of the model’s Q values for contralateral and ipsilateral choices. **d**) Surgical schematic for recording with optical fibers from the GCaMP6f terminals originating from VTA/SN. Projections were determined using viral traces. (**e**) Sample GCaMP6f traces from VTA/SN::DMS terminals and a GFP control animal. **(f, g)** Previous work has reported contralateral choice selectivity in DMS DA terminals (Parker et al. 2016) when the signals are time-locked to nose poke (**f**) and lever presentation (**g**). Colored fringes represent +/- 1 standard error.

	25th Percentile	50th Percentile (median)	75th Percentile
Alpha (learning rate)	0.205782	0.283441	0.357970
Beta (inverse temperature)	0.990275	1.058405	1.204639
Stay	0.883670	0.945385	1.008465

Table 1: **Fitted Parameters for Q-learning model from PyStan.** 25th, 50th, and 75th percentile of the alpha, beta, and stay parameters of the Q-learning mixed effect model. These are the the group-level parameters that reflect the distribution of the subject-level parameters.

Predictions of Contralateral and Chosen Value Models

In order to examine how value-related activity might (or might not) explain seemingly movement-related activity, we introduced two hypothetical frames of reference by which the DMS DA neurons' activity may be modulated by predicted value during trial events prior to the outcome: the DA signals could be modulated by the value of the contralateral option (relative to ipsilateral; **Figure 2a**) or by the value of the chosen option (relative to unchosen; **Figure 2b**). Note that both of these modulations could be understood as the anticipatory component (occasioned at lever presentation) of a temporal difference RPE, with respect to the respective action's value.

The first possibility is modulation by the value of the contralateral (relative to ipsilateral) action (**Figure 2a**; such signals have been reported in human neuroimaging, Gershman et al., 2009, Palmenteri et al. 2009; but not previously to our knowledge examined in DA unit recordings in animals). The motivation for this hypothesis is that, if neurons in DMS participate in contralateral movements, such a side-specific error signal would be appropriate for teaching them when those movements are valuable. In this case, the relative value of the contralateral (versus ipsilateral) choice modulates signals, regardless of whether the choice is contralateral or ipsilateral. Thus, when the DA signals are broken down with respect to both the action chosen and its value, the direction of value modulation would depend on the choice: signals are highest for contralateral choices when these are relatively most valuable, but lowest for ipsilateral choices when *they* are most valuable (because in this case, contralateral choices will be relatively less valuable). Assuming mice tend to choose the option they expect to deliver more reward, such signals would be larger, on average, during contralateral choices than ipsilateral ones (**Figure 2a**), which could in theory explain the contralateral choice selectivity that we observed (**Figure 1f,g**).

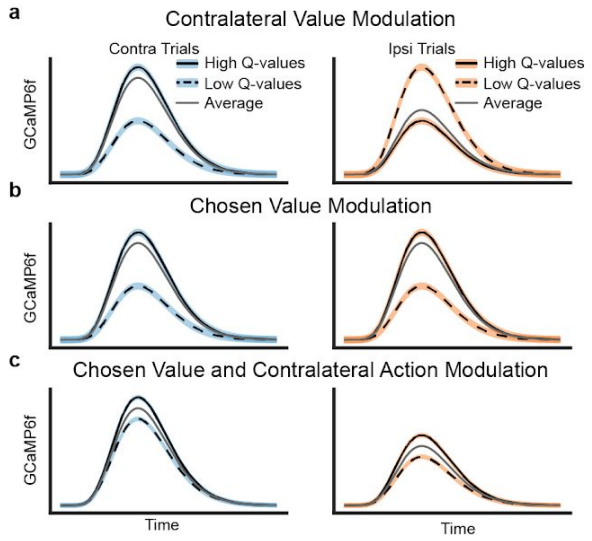

Figure 2: Schematics of possible types of value modulation at lever presentation. Trials here are divided based on Q values of chosen minus unchosen action. **(a)** Contralateral value modulation theory postulates that the signals are selective for the *value* of the contralateral action (relative to ipsilateral value) instead of the action itself. This means that the direction of value modulation should be flipped for contralateral versus ipsilateral choices. Since mice would more often choose an option when its value is higher, the average GCaMP6f signals would be higher for contralateral than ipsilateral choices. **(b)** Alternatively, the signals may be modulated by the value of the chosen action, resulting in similar value modulation for contralateral and ipsilateral choice. This type of value modulation will not in itself produce contralateral selectivity seen in previous results. (**c**) However, if the signals were modulated by the chosen value and the contralateral choice, the averaged GCaMP6f would exhibit the previously seen contralateral selectivity.

The second possibility is that value modulation is relative to the chosen (versus unchosen) option (**Figure 2b**). This corresponds to the standard type of "critic" RPE most often invoked in models of DA: that is, RPE with respect to the overall value of the current state or situation (where that state reflects any choices previously made), and not specialized to a particular class of action. Indeed, human neuroimaging studies have primarily reported correlates of the value of the chosen option in DAtarget areas (Daw et al., 2006; Boorman et al., 2009; Li & Daw, 2011), and this also has been observed in primate DAneurons (Morris et al., 2006).

If DMS-projecting DA neurons indeed display chosen value modulation (**Figure 2b**), rather than contralateral value modulation, the value modulation for both contralateral and ipsilateral choices would be similar. In this case, value modulation could not in itself account for the neurons' elevated activity during contralateral trials, which we have previously observed(**Figure 1f,g**). Therefore, to account for contralateral choice preference, one would have to assume DA neurons are also selective for the contralateral action itself (unrelated to their value modulation; **Figure 2c**).

DA in dorsomedial striatum is modulated by chosen value, not contralateral value

Next, we determined which type of value modulation better captured the signal in DA neurons that project to DMS by comparing the GCaMP6f signal in these neurons for high and low value trials. We focused on the lever presentation since this event displayed a clear contralateral preference (**Figure 1g**). As a simple and objective proxy for the value of each action (i.e., the component of the RPE at lever presentation for each action), we compared signals when the animal was rewarded (high value), or not (low value), on the previous trial. (To simplify interpretation of this comparison, we only included trials in which the mice made the same

choice as the preceding trial, which accounted for 76.6% of the trials.) The traces (**Figure 3a**) indicated that the VTA/SN::DMS terminals were modulated by the previous trial's reward. The value-related signals reflected chosen value – responding more when the previous choice was rewarded, whether contralateral or ipsilateral – and therefore did not explain the movement-related effect. This indicates that the DMS-projecting DA neurons represent both chosen value and movement direction (similar to **Figure 2c**). The effect of contralateral action modulation was also visible in individual, non-z-scored data in both VTA/SN::DMS terminals (**Figure 3-Figure Supplement 1**) and VTA/SN::DMS cell-bodies (**Figure 3-Figure Supplement 2)**.

We repeated this analysis using trial-by-trial Q values extracted from the model, which we reasoned should reflect a finer grained (though more assumption-laden) estimate of the action's value. (For this analysis, we were able to include both stay and switch trials.) Binning trials by chosen (minus unchosen) value, a similar movement effect and value gradient emerged as we have seen with the previous trial outcome analysis (**Figure 3b**). Trials with higher Q values had larger GCaMP6f signals, regardless which side was chosen, again suggesting that VTA/SN::DMS terminals were modulated by the expected value of the chosen (not contralateral) action, in addition to being modulated by contralateral movement.

To quantify these effects statistically, we used a linear mixed effects regression at each of time point of the time-locked GCaMP6f. The explanatory variables included the action chosen (contra or ipsi), the differential Q values (oriented in the reference frame suggested by the data, chosen minus unchosen), the value by action interaction, and an intercept (**Figure 3c**). The results verify significant effects of both movement direction and action value; that is, although a significant value effect is seen, it does not explain away the movement effect. Furthermore, the appearance of a consistent chosen value effect across both ipsilateral and contralateral choices is reflected in a significant value effect and no significant interaction during the period when action and value coding are most prominent (0.25 - 1 seconds after lever presentation), as would have been predicted by the contralateral value model. (There is a small interaction between the variables earlier in the trial, before 0.25 seconds, reflecting small differences in the magnitude of value modulation on contralateral versus ipsilateral trials.) Conversely, when the regression is re-estimated in terms of contralateral value rather than chosen value, a sustained, significant interaction does emerge, providing formal statistical support for the chosen value model; see **Figure 3-Figure Supplement 3.**

We performed the same value modulation analyses on the cell bodies, rather than terminals, of VTA/SN::DMS neurons (**Figure 3d-f**). This was motivated by the possibility that there may be changes in neural coding between DA cell bodies and terminals due to direct activation of DA terminals. In this case, we found very similar modulation by both chosen value and contralateral movement in both recording locations.

To verify the robustness of these findings, we conducted further followup analyses. In one set of analyses, we investigated to what extent the DA signals might be tied to particular events other

than the lever presentation. First, we repeated our analyses on DA signals time-locked to nose poke event (**Figure 3-Figure Supplement 4**), and found the same basic pattern of effects. The effect is still clearest close to the average lever presentation latency, suggesting that the modulation of DA signals is more closely related to lever presentation. To more directly verify that our conclusions are independent of the specific choice event alignment, we fitted a linear regression model with kernels capturing the contribution of three three different events (Nose Poke, Lever Presentation, and Lever Press) simultaneously (**Figure 3-Figure Supplement 5**). The results of this multiple event regression were consistent with the simpler single-event regression in **Figure 3a, d**.

Next, we examined a few other factors that might have affected movement-specific activity. Taking advantage of the fact that the VTA/SN::DMS cell-bodies data had recordings from both hemispheres in three animals, we directly compared signals across hemispheres in individual mice and observed that the side-specific effects reversed within-animal (**Figure 3-Figure Supplement 6**). This speaks against the possibility that they might reflect animal-specific idiosyncrasies such as side biases. Finally, we considered whether the contralateral action modulation might in part reflect movement vigor rather than action value. We addressed this by repeating the analysis in **Figure 3c,f,** but including as an additional covariate the log lever-press latency, as a measure of the action's vigor. For both VTA/SN::DMS terminals and cell-bodies data, the lever-press latency was not a strong predictor for GCaMP6f signals, and the effect of the original predictors largely remained the same (**Figure 3-Figure Supplement 7**).

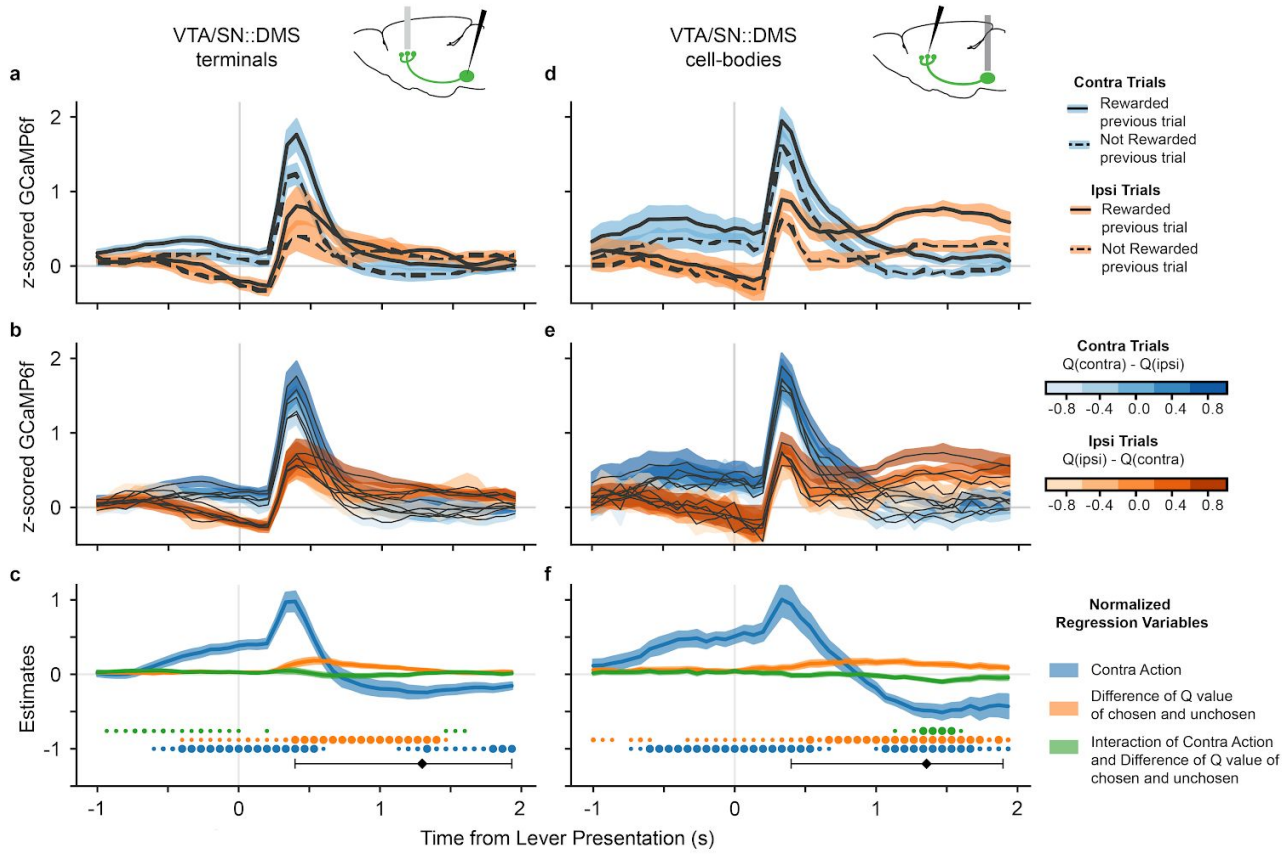

Figure 3: DA neurons that project to DMS are modulated by both chosen value and movement direction. (a) GCaMP6f signal time-locked to lever presentation for contralateral trials (blue) and ipsilateral trials (orange), as well as rewarded (solid) and non-rewarded previous trial (dotted) from VTA/SN::DMS terminals. Colored fringes represent +/- 1 standard error from activity averaged across recording sites (n = 12). **(b)** GCaMP6f signal for contralateral trials (blue) and ipsilateral trials (orange), and further binned by the difference of Q values of chosen and unchosen action. Colored fringes represent +/- 1 standard error from activity averaged across recording sites (n = 12). **(c)** Mixed effect model regression on each datapoint from 3 seconds of GCaMP6f traces. Explanatory variables include the action of the mice (blue), the difference in Q values for chosen and unchosen actions (orange), their interaction (green), and an intercept. Colored fringes represent +/- 1 standard error from estimates (n = 12 recording sites). Black diamond represents the average latency for mice pressing the lever, with the error bars showing the spread of 80% of the latency values. Dots at bottom mark timepoints when the corresponding effect is significantly different from zero at p<.05 (small dot), p<.01 (medium dot), p<.001 (large dot). P values were corrected with Benjamini Hochberg procedure. **(d-f)** Same as **(a-e),** except VTA/SN::DMS cell body averaged across recording sites (n = 7) instead of terminals.

Direction of movement predicts DMS DA signals

An additional observation supported the interpretation that the contralateral choice selectivity in DMS-projecting DA neurons is related to the direction of movement, and not the value of the choice. When the signals are time-locked to the lever press itself, there is a reversal of the

signal selectivity between contralateral and ipsilateral trials, shortly after the lever press (**Figure 4**). Although body tracking is not available, this event coincided with a reversal in the animal's physical movement direction, from moving toward the lever from the central nosepoke before the lever press, to moving back to the central reward port after the lever press. In contrast, there is no reversal in the value modulation at the time of the lever press. The fact that the side-specific modulation (and not the value modulation) followed the mice's movement direction during the trial further indicates that movement direction explains the choice selectivity in these DA neurons, and resists explanation in terms of RPE-related signaling.

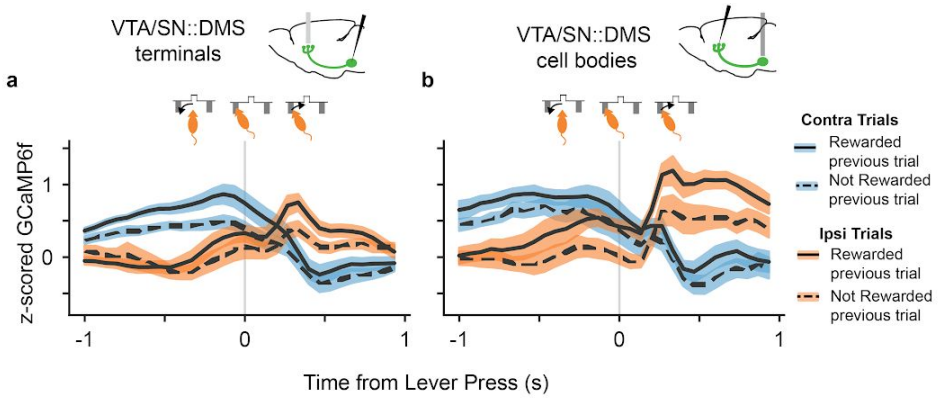

Figure 4: DA neurons that project to DMS reverse their choice selectivity after the lever press, around the time the mice reverse their movement direction. **(a)** GCaMP6f signal from VTA/SN::DMS terminals time-locked to the lever press, for contralateral choice trials (blue) and ipsilateral choice trials (orange), as well as rewarded (solid) and non-rewarded previous trial (dotted). The GCaMP6f traces for each choice crosses shortly after the lever-press, corresponding to the change in the mice's head direction around the time of the lever press (shown schematically above the plot). Colored fringes represent +/- 1 standard error from activity averaged across recording sites (n = 12). **(b)** Same as **(a),** except VTA/SN::DMS cell body averaged across recording sites (n = 7) instead of terminals.

Discussion

Recent reports of qualitatively distinct DA signals - movement and RPE-related - have revived perennial puzzles about how the system contributes to both movement and reward, and more specifically raise the question whether there might be a unified computational description of both components in the spirit of the classic RPE models (Parker et al. 2016; Berke 2018; Coddington and Dudman 2018; Syed et al. 2016). Here we introduce and test one possible route to such a unification: action-specific RPEs, which could explain seemingly action-selective signals as instead reflecting RPE related to the value of those actions. To investigate this possibility, we dissected movement direction and value selectivity in the signals of terminals and cell bodies of DMS-projecting DA neurons (**Figure 3**). Contrary to the hypothesis that lateralized movement-related activity might reflect a RPE for contralateral value, multiple lines of evidence clearly indicated that the neurons instead contain distinct movement- and value-related signals, tied to different frames of reference. We did observe value-related signals preceding and following the lever press, which we did not previously analyze in the DMS signal and which are consistent with the anticipatory component of a classic RPE signal (Parker et al. 2016). But because these were modulated by the value of the chosen action, not the contralateral one,

they cannot explain the side-specific movement selectivity. The two signals also showed clearly distinct time courses; in particular, the side selectivity reversed polarity following the lever press, but value modulation did not.

Our hypothesis that apparently movement-related DA correlates might instead reflect action-specific RPEs (and our approach to test it by contrasting chosen vs. action-specific value) may also be relevant to other reports of DAergic movement selectivity. For example, Syed et al. recently reported that DA release in the nucleus accumbens (NAcc) was elevated during “go”, rather than “no-go”, responses, alongside classic RPE-related signals (Syed et al. 2016). This study leaves open a question analogous to the one we raise about Parker’s (Parker et al. 2016) DMS results: could NAcc DA instead reflect an RPE specific for “go” actions? This possibility would be consistent with the structure’s involvement in appetitive approach and invigoration (Parkinson et al. 2002), and might unify the RPE- and “go”-related activity reported there via an action-specific RPE (argument analogous to **Figure 2a)**. The analyses in the Syed et al. study did not formally compare chosen- vs. action-specific value, and much of the reward-related activity reported there appears consistent with either account (Syed et al. 2016). However, viewed from the perspective of our current work, the key question becomes whether the value-related DA signals on “go” cues reverses for “no-go” cues, as would be predicted for an action-specific RPE. There is at least a hint (albeit significant only at one timepoint in Syed et al.’s Supplemental Figure 9E) that it does not do so (Syed et al. 2016). This suggests that NAcc may also have parallel movement-specific and chosen value signals, which would be broadly confirmatory for our parallel conclusions about DMS-projecting DA neurons.

The RPE account of the DA signal has long held out hope for a unifying perspective on the system’s dual roles in movement and reward by proposing that the system’s reward-related signals ultimately affect movement indirectly, either by driving learning about movement direction preferences (Montague, Dayan, and Sejnowski 1996) or by modulating motivation to act (Niv et al. 2007). This RPE theory also accounts for multiple seemingly distinct components of the classic DA signal, including anticipatory and reward-related signals, and signals to novel neutral cues. However, the present analyses clearly show that side-specific signals in DMS resist explanation in terms of an extended RPE account, and may instead simply reflect planned or ongoing movements.

Specifically, our results are consistent with the longstanding suggestion that DA signals may be important for directly initiating movement. Such a signal may elicit or execute contralateral movements via differentially modulating the direct and indirect pathways out of the striatum (Alexander and Crutcher 1990; Collins and Frank 2014; DeLong 1990). The relationship between unilateral DA activity and contralateral movements is also supported by causal manipulations. For instance, classic results demonstrate that unilateral 6-hydroxydopamine (6-OHDA) lesions increase ipsilateral rotations (Costall, Naylor, and Pycock 1976; Ungerstedt and Arbuthnott 1970). Consistent with those results, a recent study reports that unilateral optogenetic excitation of midbrain DA neurons in mice led to contralateral rotations developed over the course of days (Saunders et al. 2018). Importantly, however, our own results are

correlational, and we cannot rule out the possibility that the particular activity we study could be related to a range of functions other than movement execution, such as planning or monitoring. Another function that is difficult to distinguish from movement execution is the motivation to move. Although motivation is a broad concept and difficult to operationalize fully, our results address two aspects of it. First, one way to quantify the motivation to act is by the action's predicted value; thus, our main result is to rule out the possibility that neural activity is better accounted for by this motivational variable. We also show that lever press latency (arguably another proxy for motivation) does not explain the DA signals (**Figure 3-Figure Supplement 7**).

Although the movement-related DA signal might be appropriate for execution, it is less clear how it might interact with the plasticity mechanisms hypothesized to be modulated by RPE aspects of the DA signal (Frank, Seeberger, and O'reilly 2004; Steinberg et al. 2013; Reynolds and Wickens 2002). For instance, how would recipient synapses distinguish an RPE component of the signal (appropriate for surprise-modulated learning) from an overlapping component more relevant to movement elicitation (Berke 2018)? We have ruled out the possibility that the activity is actually a single RPE for action value, but there may still be other sorts of plasticity that might be usefully driven by a purely movement-related signal. One possibility is that plasticity in the dorsal striatum itself follows different rules, which might require an action rather than a prediction error signal (Saunders et al. 2018; Yttri and Dudman 2016) For instance, it has been suggested that some types of instrumental learning are correlational rather than error-driven (Doeller, King, and Burgess 2008) and, more specifically, an early model of instrumental learning ((Guthrie 1935) recently revived by (Miller, Shenhav, and Ludvig 2019) posits that stimulus-response habits are not learned from an action's rewarding consequences, as in RPE models, but instead by directly memorizing which actions the organism tends to select in a situation. Although habits are more often linked to adjacent dorsolateral striatum (Yin, Knowlton, and Balleine 2004), a movement signal of the sort described here might be useful to drive this sort of learning. Investigating this suggestion will likely require new experiments centered around causal manipulations of the signal. Overall, our results point to the need for an extended computational account that incorporates the movement direction signals as well as the RPE ones.

Another striking aspect of the results is the co-occurrence of two distinct frames of reference in the signal. Lateralized movement selectivity tracks choices contralateral versus ipsilateral of the recorded hemisphere –appropriate for motor control–, but the value component instead relates to the reward expected for the chosen, versus unchosen, action. This value modulation by the chosen action is suitable for a classic RPE for learning "state" values (since overall value expectancy at any point in time is conditioned on the choices the animal has made; (Morris et al. 2006), and also consistent with the bulk of BOLD signals in human neuroimaging, where value-related responding throughout dopaminergic targets tends to be organized on chosen-vs-unchosen lines (Daw et al. 2006; Boorman et al. 2009; Li and Daw 2011; O'Doherty 2014).

At the same time, there have been persistent suggestions that given the high dimensionality of an organism's action space, distinct action-specific error signals would be useful for learning about different actions (Russell and Zimdars 2003; Frank and Badre 2012; Diuk et al. 2013) or types of predictions (Gershman and Schoenbaum 2017; Lau, Monteiro, and Paton 2017). Along these lines, there is evidence from BOLD neuroimaging for contralateral error and value signals in the human brain (Gershman, Pesaran, and Daw 2009; Palminteri et al. 2009). Here, we have shown how a similar decomposition might explain movement-related DA signals, and also clarified how this hypothesis can be definitively tested. Although the current study finds no evidence for such laterally decomposed RPEs in DMS, the decomposition of error signals remains an important possibility for future work aimed at understanding heterogeneity of dopamine signals, including other anomalous features like ramps (Howe et al. 2013; Berke 2018; Gershman 2014; Hamid et al. 2016; Engelhard et al. 2018; da Silva et al. 2018). Recent studies, for instance, have shown that midbrain DA neurons may also encode a range of behavioral variables, such as the mice's position, their velocity, their view-angle, and the accuracy of their performance (Howe et al. 2013; da Silva et al. 2018; Engelhard et al. 2018). Our modeling provides a framework for understanding how these DA signals might be interpreted in different reference frames and how they might ultimately encode some form of RPEs with respect to different behavioral variables in the task.

Interestingly, our results were consistent across both recording sites with DMS-projecting DA neurons: the cell bodies and the terminals (**Figure 3d-f, Figure 4b**). This indicates that the movement selectivity is not introduced in DA neurons at the terminal level, e.g. via striatal cholinergic interneurons or glutamatergic inputs (Kosillo et al. 2016).

An important limitation of the study is the use of fiber photometry, which assesses bulk GCaMP6f signals at the recording site rather than resolving individual neurons. Thus it remains possible that individual neurons do not multiplex the two signals we observe, and that they are instead segregated between distinct populations. Future work should use higher resolution methods to examine these questions at the level of individual DA neurons. A related limitation of this study is the relatively coarse behavioral monitoring; notably, we infer that the reversal in selectivity seen in **Figure 4** reflects a change in movement direction, but head tracking would be required to verify this more directly. More generally, future work with finer instrumentation could usefully dissect signal components related to finer-grained movements, and examine how these are related to (or dissociated from) value signals.

Acknowledgments

We thank the entire Witten and Daw labs for comments, advice and support on this work. I.B.W. is a New York Stem Cell Foundation—Robertson Investigator.

Methods

Mice and Surgeries

This article reports new analysis on data originally reported by (Parker et al. 2016). We briefly summarize the methods from that study here. This article reports on data from 17 male mice expressing Cre recombinase in the tyrosine hydroxylase promoter (*Th*$^{IRES\text{-}Cre}$), from which GCaMP6f recordings were obtained from DA neurons via fiber photometry.

In the case of DA terminal recordings, Cre-dependent GCaMP6f virus (AAV5-CAG-Flex-GCamp6f-WPRE-SV40; UPenn virus core, injected titer of 3.53 × 1012 pp per ml) was injected into the VTA/SNc, and fibers were placed in the DMS (M–L ± 1.5, A–P 0.74 and D–V −2.4 mm), with one recording area per mouse (n = 12 recording sites). The recording hemisphere was counterbalanced across mice. The mice were recorded bilaterally, with the second site in nucleus accumbens, which is not analyzed in this paper.

In the case of VTA/SN::DMS cell body recordings, Cre-dependent GCaMP6f virus (AAV5-CAG-Flex-GCamp6f-WPRE-SV40; UPenn virus core, injected titer of 3.53 × 1012 pp per ml) was injected into the DMS, and fibers were placed on the cell bodies in VTA/SNc (M–L ± 1.4, A–P 0.74, D–V −2.6 mm), enabling recordings from retrogradely labeled cells (n=4 mice). Three of the mice were recorded from both hemispheres, providing a total of n = 7 recording sites.

One mouse was used for the GFP recordings as a control condition for VTA/SNc::DMS terminals recordings (**Figure 1e**).

Instrumental Reversal Learning Task

The recordings were obtained while the mice performed a reversal learning task in an operant chamber with a central nose poke, retractable levers on each side of the nose poke, and reward delivery in a receptacle beneath the central nose poke.

Each trial began with the illumination of the center nose port. After the mouse entered the nose port, the two levers were presented with a delay that varied between 0-1 seconds. The mouse then had 10 seconds to press a lever, otherwise the trial was classified as an abandoned trial and excluded from analysis (this amounted to <2 % of trials for all mice). After the lever-press, an additional random 0-1 second delay (0.1 second intervals, uniform distribution) preceded either CS- with no reward delivery or CS+ with a 4µl reward of 10% sucrose in H_20. Reward outcomes were accompanied by different auditory stimulus: 0.5 seconds of white noise for CS- and 0.5 seconds of 5 kHz pure tone for CS+. Every trial ended with a constant 3 seconds inter-trial delay.

For the reversal learning, each of the levers either had a high probability for reward (70%) or low probability for reward (10%). Throughout the session, the identity of the high probability lever changed in a pseudorandom schedule; specifically, each block consisted of at least 10 rewarded trials plus a random number of trials drawn from a Geometric distribution of p = 0.4 (mean 2.5). On average, there were 23.23 +/- 7.93 trials per block and 9.67 +/- 3.66 blocks per session. Both reported summary statistics are mean +/- standard deviation.

Data processing

All fiber photometry recordings were acquired at 15 Hz. 2-6 recording sessions were obtained per recording site (1 session/day), and these recordings were concatenated across session for all analyses. On average, we had 1307.0 ± 676.01 trials per mouse (858.09 ± 368.56 trials per mouse for VTA/SN::DMS Terminals recordings and 448.91 ± 455.61 trials per mouse for VTA/SN::DMS Cell-bodies recordings).

The signal from each recording site were post-processed with a high-pass FIR filter with a passband of 0.375 Hz, stopband of 0.075 Hz, and a stopband attenuation of 10 dB to remove baseline fluorescence and correct drift in baseline. We derived dF/F by dividing the high-pass filtered signal by the mean of the signal before high-pass filtering. We then z-scored dF/F for each recording site, with the the mean and standard error calculated for the entire recording from each site.

The VTA/SN::DMS terminals data consisted of 10108 total trials across 12 recording sites, and VTA/SN::DMS cell-bodies consisted of 4938 total trials across 7 recording sites.

Q Learning Mixed Effect Model

We fitted a trial-by-trial Q-learning mixed effect model to the behavioral data from each of the 12 mice on all recording sites, and combined data across mice with a hierarchical model. The model was initialized with a Q value of 0 for each action and updated at each trial according to:

$$Q_{t+1}(c_t) = Q_t(c_t) + \alpha(r_t - Q_t(c_t))$$

where Q is the value for both options, c_t is the option chosen on trial *t* (lever either contralateral or ipsilateral to recording site), and 0 <= α <= 1 is a free learning rate parameter. The subject's probability to choose choice *c* was then given by a softmax equation:

$$P(c_t = c) \propto exp(\beta \cdot Q_t(c) + stay \cdot I(c, c_{t-1}))$$

where β is a free inverse temperature parameter, *stay* is a free parameter encoding how likely the animal will repeat its choice from the last trial, and *I* is a binary indicator function for choice repetition (1 if *c* was chosen on the previous trial; 0 otherwise). The three free parameters of the

model were estimated separately for each subject, but jointly (in a hierarchical random effects model) with group-level mean and variance parameters reflecting the distribution, over the population, of each subject-level parameter.

The parameters were estimated using Hamiltonian Monte Carlo, as implemented in the Stan programming language (version 2.17.1.0; (Carpenter et al. 2017)). Samples from the posterior distribution over the parameters were extracted using the Python package PyStan (Carpenter et al. 2017). We ran the model with 4 chains of 1,000 iterations for each (of which the first 250 were discarded for burn-in), and the parameter adapt_delta set to 0.99. We verified convergence by visual inspection and by verifying that the potential scale reduction statistic Rhat (Gelman and Rubin 1992) was close to 1.0 (<0.003 for all parameters) (**Table 1)**.

We used the sampled parameters to compute per-trial Q values for each action, trial, and mouse. We calculated the difference between the Q values of the chosen action and unchosen action for each trial. We binned the difference of these Q values for each trial and plotted the average GCaMP6f time-locked to lever presentation for each bin (**Figure 3b, e**).

Regression Model

In **Figure 3c,f**, we performed a linear mixed effect model regression to predict GCaMP6f signal at each time point based on Q-values, choice (contralateral vs ipsilateral), their interaction, and an intercept. We took the difference of Q values for the chosen vs unchosen levers, then we standardized the difference of Q values for each mouse and each recording site. GCaMP6f was time-locked to lever presentation, regressing to data points 1 second before and 2 seconds after the time-locked event for 45 total regressions. The regression, as well as the calculation of p values, was performed with the MixedModels package in Julia (Bezanson et al. 2014). The p values were corrected for false discovery rate over the ensemble of timepoints for each regression variable separately, using the procedure of Benjamini and Hochberg (Benjamini and Hochberg 1995) via the MultipleTesting package in Julia (Bezanson et al. 2014).

Multiple event Kernel Analysis

In **Figure 3-Figure Supplement 5,** we fitted a linear regression model to determine the contributions to the ongoing GCaMP6f signal of three simultaneously modeled events (Nose poke, lever presentation, lever press). To do this, we used kernels, or sets of regressors covering a series of time lags covering the period from 1 second before to 2 seconds after each event. Each event had four kernels, corresponding to the four conditions from **Figure 3a, c** (all combinations of contralateral vs ipsilateral trials and previous reward vs no previous reward trials). We solved for the kernels by regressing the design matrix against GCaMP6f data using least squares in R with the rms package (Harrell 2018). The standard error (colored fringes) was calculated using rms' robcov (cluster robust-covariance) function to correct for violations of ordinary least squares assumptions due to animal-by-animal clustering in the residuals.

Supplementary Figures

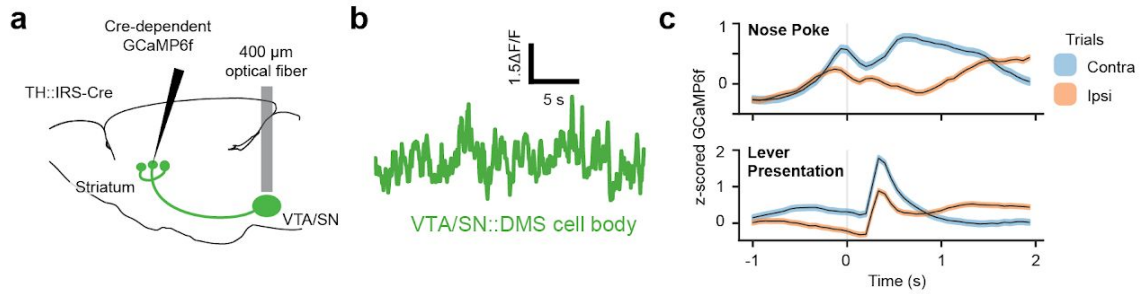

Figure 1-Figure Supplement 1: Recording from VTA/SN::DMS cell bodies (n = 7 recording sites) (**a**) Surgical schematic for recording with optical fibers from the GCaMP6f VTA/SN::DMS cell-bodies. Projections were determined using viral traces. (**b**) Sample GCaMP6f traces from VTA/SN::DMS cell bodies. **(c, d)** Contralateral choice selectivity was also observed in DMS DA cell bodies when the signals were time-locked to nose poke (**c**) and lever presentation (**d**). Colored fringes represent +/- 1 standard error from activity averaged across recording sites (n = 7).

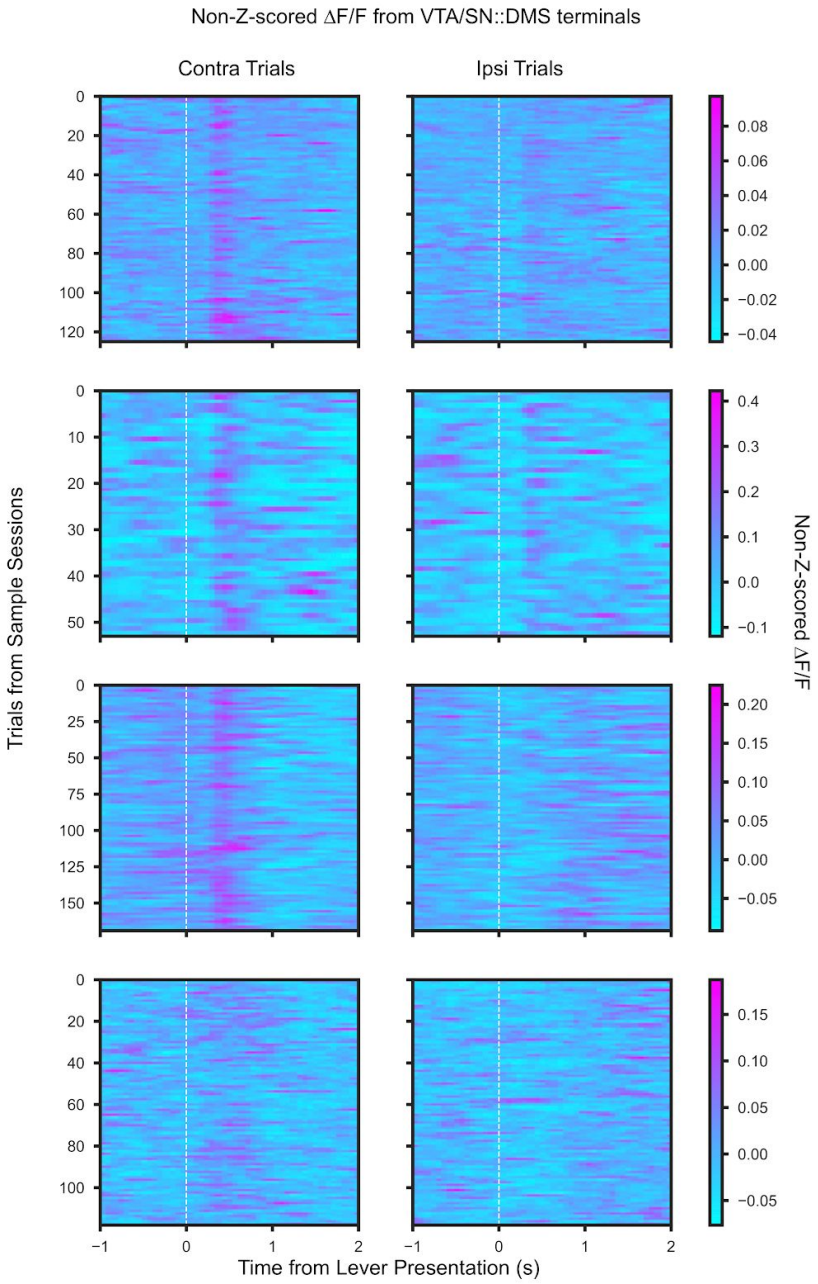

Figure 3-Figure Supplement 1: Four Examples of non-Z-scored Individual Sessions of Photometry Data from VTA/SN::DMS Terminals. Sample, not Z-scored ΔF/F recording from VTA/SN::DMS Terminal. Each row is an example session from a different mouse. Traces are time-locked to the lever presentation for contralateral trials (**left column**) and ipsilateral trials (**right column**). White dotted vertical line indicate lever presentation. Colorbars are provided for each row for each example session.

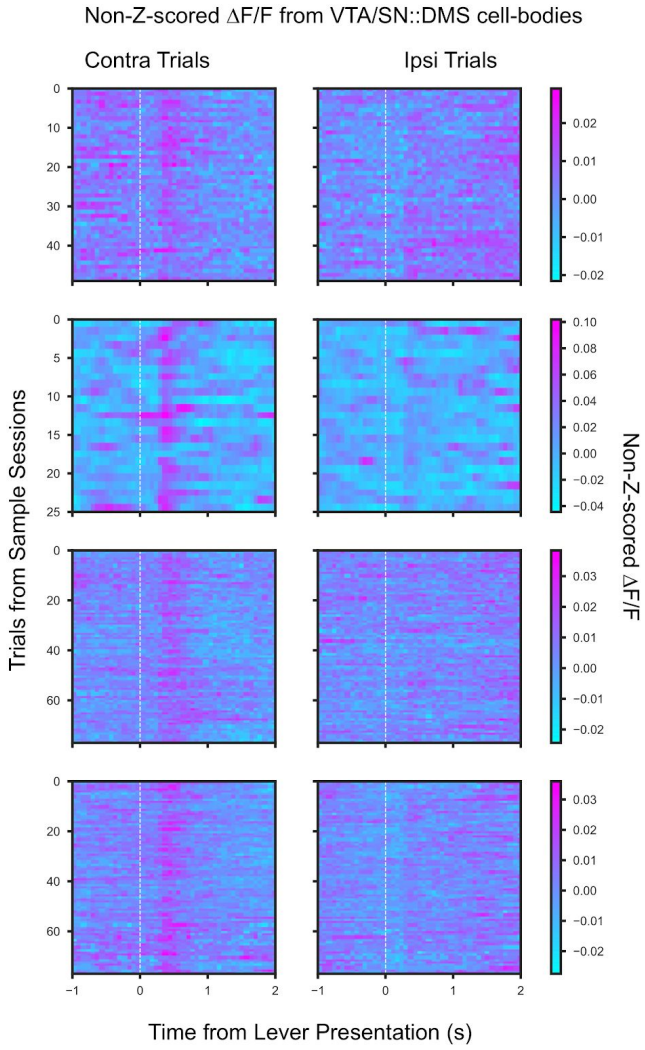

Figure 3-Figure Supplement 2: Four Examples of non-Z-scored Individual Sessions of Photometry Data from VTA/SN::DMS Cell-Bodies. Sample, not Z-scored ΔF/F recording from VTA/SN::DMS Cell-bodies. Each row is an example session from a different mouse. Traces are time-locked to the lever presentation for contralateral trials (**left column**) and ipsilateral trials (**right column**). White dotted vertical line indicate lever presentation. Colorbars are provided for each row for each example session.

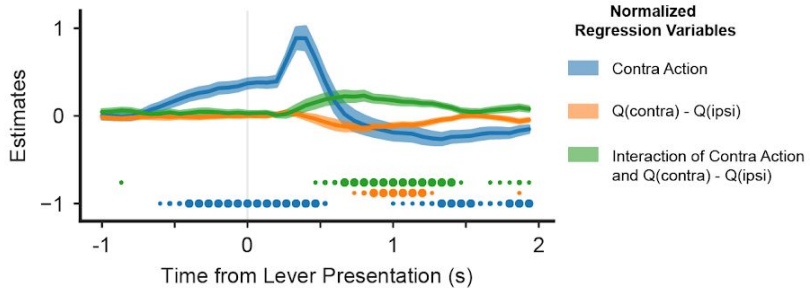

Figure 3-Figure Supplement 3: Mixed effect model regression on GCaMP6f traces of VTA/SN::DMS terminals (n = 12 recording sites) using Q values of contralateral minus ipsilateral. Same analysis as **Figure 3c**, except explanatory variables include the action of the mice (blue), the difference in Q values for contralateral and ipsilateral choices (orange), their

interaction (green), and an intercept. Colored fringes represent +/- 1 standard error from estimates (n = 12 recording sites). Dots at bottom mark timepoints where the corresponding effect is significantly different from zero at p<.05 (small dot), p<.01 (medium dot), p<.001(large dot). P values were corrected with Benjamini Hochberg procedure.

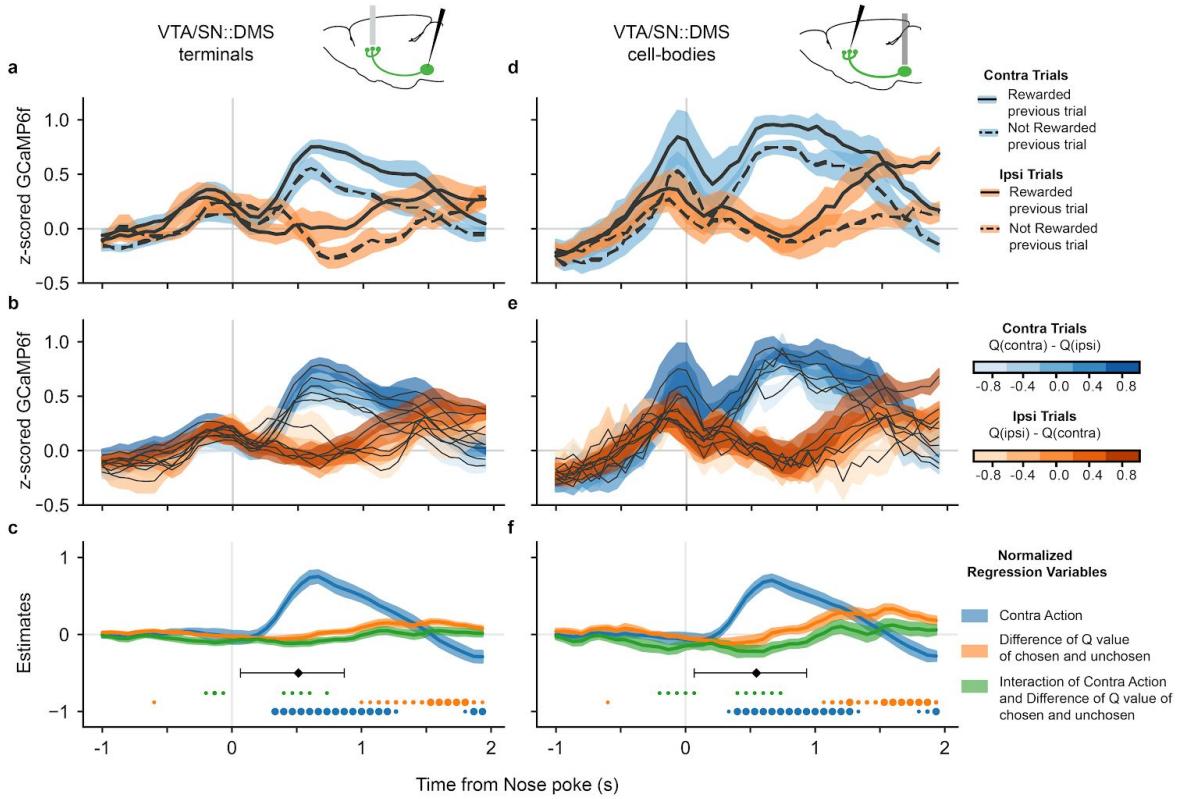

Figure 3-Figure Supplement 4: Analysis of DA signals time-locked to nose poke. (a) GCaMP6f signal time-locked to nose poke for contralateral trials (blue) and ipsilateral trials (orange), as well as rewarded (solid) and non-rewarded previous trial (dotted) from VTA/SN::DMS terminals. Colored fringes represent +/- 1 standard error from activity averaged across recording sites (n = 12). **(b)** GCaMP6f signal for contralateral trials (blue) and ipsilateral trials (orange), and further binned by the difference of Q values of chosen and unchosen action. Colored fringes represent +/- 1 standard error from activity averaged across recording sites (n = 12). **(c)** Mixed effect model regression on each datapoint from 3 seconds of GCaMP6f traces. Explanatory variables include the action of the mice (blue), the difference in Q values for chosen vs unchosen actions (orange), their interaction (green), and an intercept. Colored fringes represent +/- 1 standard error from estimates (n = 12 recording sites). Black diamond represents the average latency for lever presentation from nose poke, with the error bars showing the spread of 80% of the latency values. Dots at bottom mark timepoints when the corresponding effect is significantly different from zero at p<.05 (small dot), p<.01 (medium dot), p<.001 (large dot). P values were corrected with Benjamini Hochberg procedure. **(d-f)** Same as **(a-e),** except VTA/SN::DMS cell body averaged across recording sites (n = 7) instead of terminals.

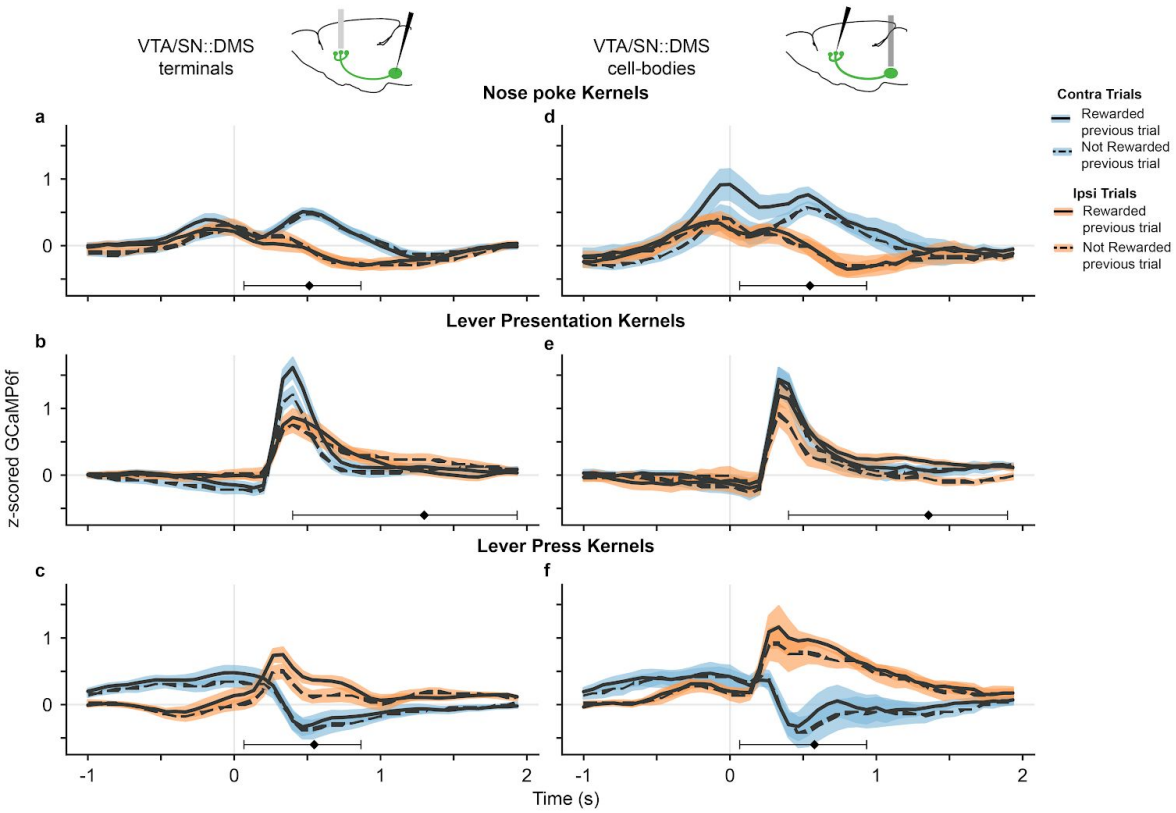

Figure 3-Figure Supplement 5: Kernels for each significant behavioral event from the multiple event kernel analysis (a) Nose poke kernel output from linear regression model using GCaMP6f from VTA/SN::DMS terminals. Each line is the kernel for a combination of contralateral (blue) and ipsilateral (orange) trials, as well as rewarded (solid) and non-rewarded (dotted) trials. Colored fringes represent +/- 1 standard error from activity averaged across recording sites (n = 12). Black diamond represents the average latency for lever presentation from nose poke with the error bars showing the spread of 80% of the latency values. **(b)** Lever presentation kernels, with the black diamond representing the average latency from lever press to lever presentation. **(c)** Lever press kernels, with the black diamond representing the average latency from CS+ or CS- to lever press. **(d-f)** Same as **(a-e),** except VTA/SN::DMS cell body averaged across recording sites (n = 7) instead of terminals.

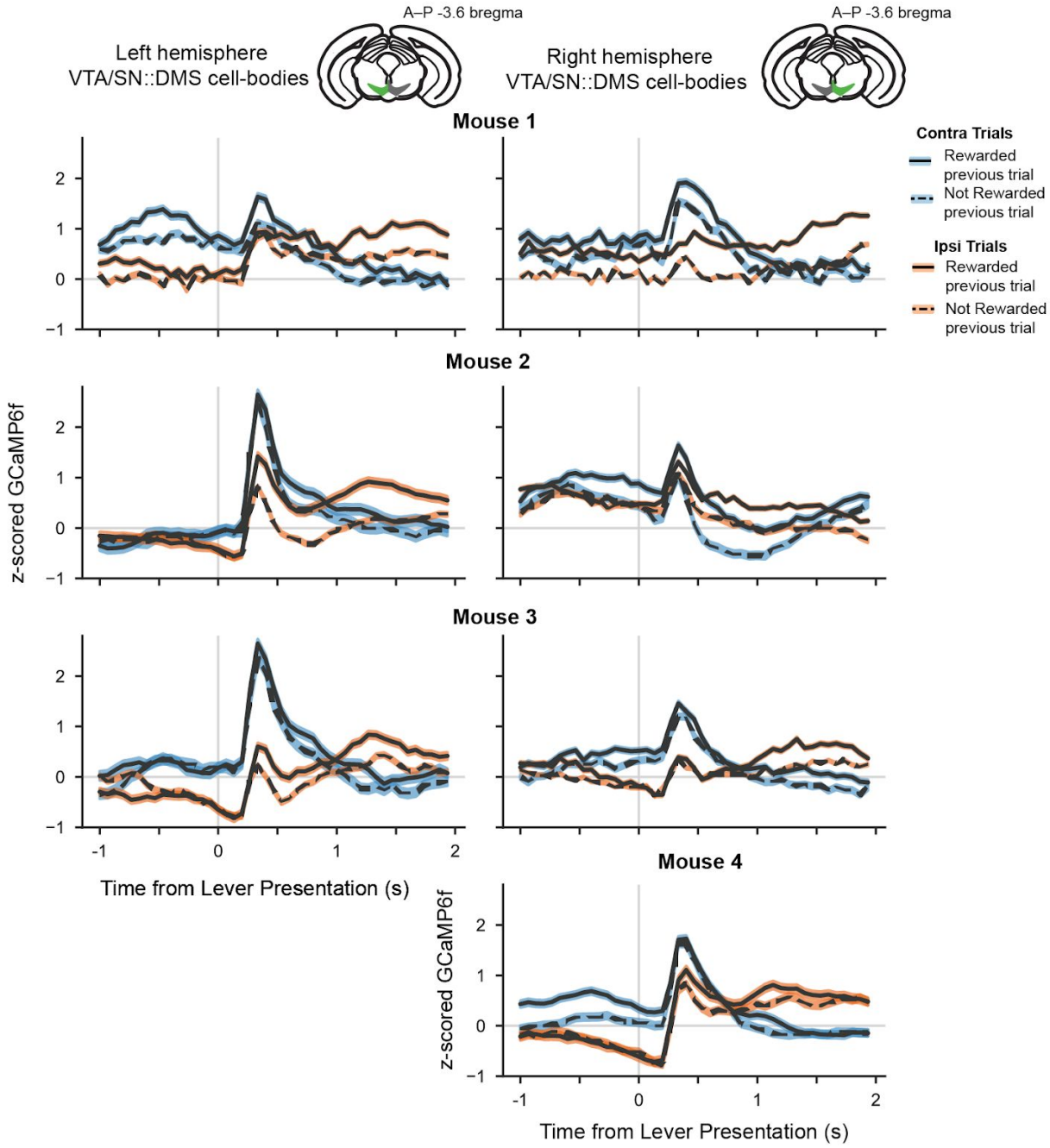

Figure 3-Figure Supplement 6: Averaged GCaMP6f signals of left and right hemispheres recordings from VTA/SN::DMS cell-bodies data (n = 4 mice, 7 recording sites). GCaMP6f signal relative to the lever presentation time for contralateral trials (blue) and ipsilateral trials (orange), as well as rewarded (solid) and non-rewarded previous trial (dotted) from VTA/SN::DMS terminals. Colored fringes represent +/- 1 standard error from activity averaged across trials. Each row represents averaged data from a distinct mouse (n = 4 total), with left and right column representing the left and right hemisphere recordings.

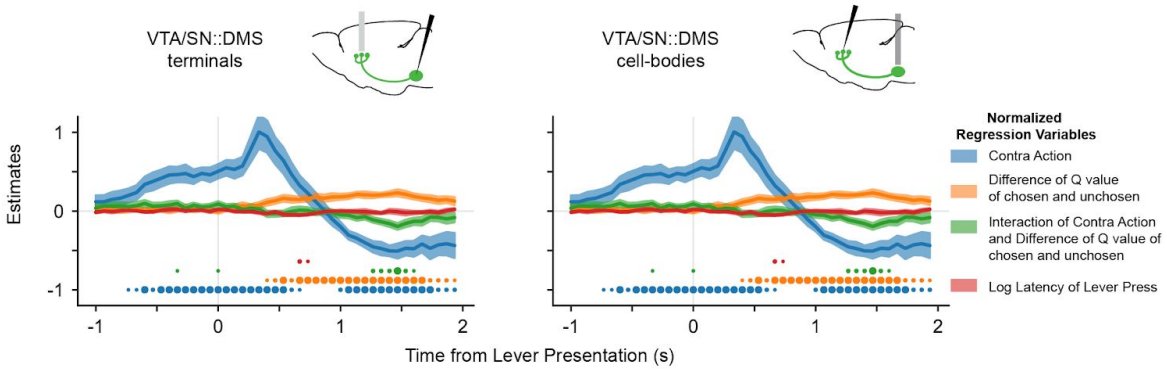

Figure 3-Figure Supplement 7: Mixed effect model regression with latency as nuisance covariate. (a) Mixed effect model regression with log latency of lever press (red) as additional nuisance covariate for VTA/SN::DMS terminal data (n = 12 recording sites). As with in **Figure 3c, f**, the mixed effect model's other explanatory variables include the action of the mice (blue), the difference in Q values for chosen vs unchosen actions (orange), their interaction (green), and an intercept. Colored fringes represent +/- 1 standard error from estimates. Dots at bottom mark timepoints when the corresponding effect is significantly different from zero at p<.05 (small dot), p<.01 (medium dot), p<.001 (large dot). P values were corrected with Benjamini Hochberg procedure. **(b)** Same as **(a),** except VTA/SN::DMS cell body averaged across recording sites (n = 7) instead of terminals.

References List

Alexander, G. E., and M. D. Crutcher. 1990. “Functional Architecture of Basal Ganglia Circuits: Neural Substrates of Parallel Processing.” *Trends in Neurosciences* 13 (7): 266–71.

Baird, L. C. 1994. “Reinforcement Learning in Continuous Time: Advantage Updating.” In *Proceedings of 1994 IEEE International Conference on Neural Networks (ICNN’94)*, 4:2448–53 vol.4.

Barter, Joseph W., Suellen Li, Dongye Lu, Ryan A. Bartholomew, Mark A. Rossi, Charles T. Shoemaker, Daniel Salas-Meza, Erin Gaidis, and Henry H. Yin. 2015. “Beyond Reward Prediction Errors: The Role of Dopamine in Movement Kinematics.” *Frontiers in Integrative Neuroscience* 9 (May): 39.

Barto, A. G., R. S. Sutton, and C. W. Anderson. 1983. “Neuronlike Adaptive Elements That Can Solve Difficult Learning Control Problems.” *IEEE Transactions on Systems, Man, and Cybernetics* SMC-13 (5): 834–46.

Barto, Andrew G. 1995. “1‘ 1 Adaptive Critics and the Basal Ganglia,.’” *Models of Information Processing in the Basal Ganglia*, 215.

Benjamini, Yoav, and Yosef Hochberg. 1995. “Controlling the False Discovery Rate: A Practical and Powerful Approach to Multiple Testing.” *Journal of the Royal Statistical Society. Series B, Statistical Methodology* 57 (1): 289–300.

Berke, Joshua D. 2018. “What Does Dopamine Mean?” *Nature Neuroscience* 21 (6): 787–93.

Bezanson, Jeff, Alan Edelman, Stefan Karpinski, and Viral B. Shah. 2014. “Julia: A Fresh Approach to Numerical Computing.” *arXiv [cs.MS]*. arXiv. http://arxiv.org/abs/1411.1607.

Boorman, Erie D., Timothy E. J. Behrens, Mark W. Woolrich, and Matthew F. S. Rushworth. 2009. “How Green Is the Grass on the Other Side? Frontopolar Cortex and the Evidence in Favor of Alternative Courses of Action.” *Neuron* 62 (5): 733–43.

Carpenter, Bob, Andrew Gelman, Matthew Hoffman, Daniel Lee, Ben Goodrich, Michael Betancourt, Marcus Brubaker, Jiqiang Guo, Peter Li, and Allen Riddell. 2017. “Stan: A Probabilistic Programming Language.” *Journal of Statistical Software, Articles* 76 (1): 1–32.

Coddington, Luke T., and Joshua T. Dudman. 2018. “The Timing of Action Determines Reward Prediction Signals in Identified Midbrain Dopamine Neurons.” *Nature Neuroscience*, October. https://doi.org/10.1038/s41593-018-0245-7.

Cohen, Jeremiah Y., Sebastian Haesler, Linh Vong, Bradford B. Lowell, and Naoshige Uchida. 2012. “Neuron-Type-Specific Signals for Reward and Punishment in the Ventral Tegmental Area.” *Nature* 482 (7383): 85–88.

Collins, Anne G. E., and Michael J. Frank. 2014. “Opponent Actor Learning (OpAL): Modeling Interactive Effects of Striatal Dopamine on Reinforcement Learning and Choice Incentive.” *Psychological Review* 121 (3): 337–66.

Costall, B., R. J. Naylor, and C. Pycock. 1976. “Non-Specific Supersensitivity of Striatal Dopamine Receptors after 6-Hydroxydopamine Lesion of the Nigrostriatal Pathway.” *European Journal of Pharmacology* 35 (2): 276–83.

Daw, Nathaniel D., John P. O’Doherty, Peter Dayan, Ben Seymour, and Raymond J. Dolan. 2006. “Cortical Substrates for Exploratory Decisions in Humans.” *Nature* 441 (7095): 876–79.

DeLong, M. R. 1990. “Primate Models of Movement Disorders of Basal Ganglia Origin.” *Trends in Neurosciences* 13 (7): 281–85.

Diuk, Carlos, Karin Tsai, Jonathan Wallis, Matthew Botvinick, and Yael Niv. 2013. “Hierarchical Learning Induces Two Simultaneous, but Separable, Prediction Errors in Human Basal

Ganglia." *The Journal of Neuroscience: The Official Journal of the Society for Neuroscience* 33 (13): 5797–5805.

Dodson, Paul D., Jakob K. Dreyer, Katie A. Jennings, Emilie C. J. Syed, Richard Wade-Martins, Stephanie J. Cragg, J. Paul Bolam, and Peter J. Magill. 2016. "Representation of Spontaneous Movement by Dopaminergic Neurons Is Cell-Type Selective and Disrupted in Parkinsonism." *Proceedings of the National Academy of Sciences of the United States of America* 113 (15): E2180–88.

Doeller, Christian F., John A. King, and Neil Burgess. 2008. "Parallel Striatal and Hippocampal Systems for Landmarks and Boundaries in Spatial Memory." *Proceedings of the National Academy of Sciences of the United States of America* 105 (15): 5915–20.

Frank, Michael J., and David Badre. 2012. "Mechanisms of Hierarchical Reinforcement Learning in Corticostriatal Circuits 1: Computational Analysis." *Cerebral Cortex* 22 (3): 509–26.

Frank, Michael J., Lauren C. Seeberger, and Randall C. O'reilly. 2004. "By Carrot or by Stick: Cognitive Reinforcement Learning in Parkinsonism." *Science* 306 (5703): 1940–43.

Gelman, Andrew, and Donald B. Rubin. 1992. "Inference from Iterative Simulation Using Multiple Sequences." *Statistical Science: A Review Journal of the Institute of Mathematical Statistics* 7 (4): 457–72.

Gershman, Samuel J., Bijan Pesaran, and Nathaniel D. Daw. 2009. "Human Reinforcement Learning Subdivides Structured Action Spaces by Learning Effector-Specific Values." *The Journal of Neuroscience: The Official Journal of the Society for Neuroscience* 29 (43): 13524–31.

Gershman, Samuel J., and Geoffrey Schoenbaum. 2017. "Rethinking Dopamine Prediction Errors." *bioRxiv*. https://doi.org/10.1101/239731.

Guthrie, E. R. 1935. *Psychology of Learning* . Oxford, England: Harper.

Harrell, Frank E., Jr. 2018. rms: Regression Modeling Strategies. R package version 5.1-2. https://CRAN.R-project.org/package=rms

Hart, Andrew S., Robb B. Rutledge, Paul W. Glimcher, and Paul E. M. Phillips. 2014. "Phasic Dopamine Release in the Rat Nucleus Accumbens Symmetrically Encodes a Reward Prediction Error Term." *The Journal of Neuroscience: The Official Journal of the Society for Neuroscience* 34 (3): 698–704.

Horvitz, J. C. 2000. "Mesolimbocortical and Nigrostriatal Dopamine Responses to Salient Non-Reward Events." *Neuroscience* 96 (4): 651–56.

Howe, Mark W., and D. A. Dombeck. 2016. "Rapid Signalling in Distinct Dopaminergic Axons during Locomotion and Reward." *Nature* 535 (7613): 505–10.

Kosillo, Polina, Yan-Feng Zhang, Sarah Threlfell, and Stephanie J. Cragg. 2016. "Cortical Control of Striatal Dopamine Transmission via Striatal Cholinergic Interneurons." *Cerebral Cortex* , August. https://doi.org/10.1093/cercor/bhw252.

Lammel, Stephan, Daniela I. Ion, Jochen Roeper, and Robert C. Malenka. 2011. "Projection-Specific Modulation of Dopamine Neuron Synapses by Aversive and Rewarding Stimuli." *Neuron* 70 (5): 855–62.

Lau, Brian, Tiago Monteiro, and Joseph J. Paton. 2017. "The Many Worlds Hypothesis of Dopamine Prediction Error: Implications of a Parallel Circuit Architecture in the Basal Ganglia." *Current Opinion in Neurobiology* 46 (October): 241–47.

Li, Jian, and Nathaniel D. Daw. 2011. "Signals in Human Striatum Are Appropriate for Policy Update rather than Value Prediction." *The Journal of Neuroscience: The Official Journal of the Society for Neuroscience* 31 (14): 5504–11.

Matsumoto, Masayuki, and Okihide Hikosaka. 2009. "Two Types of Dopamine Neuron Distinctly Convey Positive and Negative Motivational Signals." *Nature* 459 (7248): 837–41.

Menegas, William, Benedicte M. Babayan, Naoshige Uchida, and Mitsuko Watabe-Uchida. 2017. “Opposite Initialization to Novel Cues in Dopamine Signaling in Ventral and Posterior Striatum in Mice.” *eLife* 6 (January). https://doi.org/10.7554/eLife.21886.

Miller, Kevin, Amitai Shenhav, and Elliot Ludvig. 2019. “Habits without Values.” *Psychological Review*, January, 067603.

Montague, P. R., P. Dayan, and T. J. Sejnowski. 1996. “A Framework for Mesencephalic Dopamine Systems Based on Predictive Hebbian Learning.” *The Journal of Neuroscience: The Official Journal of the Society for Neuroscience* 16 (5): 1936–47.

Morris, Genela, Alon Nevet, David Arkadir, Eilon Vaadia, and Hagai Bergman. 2006. “Midbrain Dopamine Neurons Encode Decisions for Future Action.” *Nature Neuroscience* 9 (8): 1057–63.

Niv, Yael, Nathaniel D. Daw, Daphna Joel, and Peter Dayan. 2007. “Tonic Dopamine: Opportunity Costs and the Control of Response Vigor.” *Psychopharmacology* 191 (3): 507–20.

O’Doherty, John P. 2014. “The Problem with Value.” *Neuroscience and Biobehavioral Reviews* 43 (June): 259–68.

O’Doherty, John P., Peter Dayan, Johannes Schultz, Ralf Deichmann, Karl Friston, and Raymond J. Dolan. 2004. “Dissociable Roles of Ventral and Dorsal Striatum in Instrumental Conditioning.” *Science* 304 (5669): 452–54.

Palminteri, Stefano, Thomas Boraud, Gilles Lafargue, Bruno Dubois, and Mathias Pessiglione. 2009. “Brain Hemispheres Selectively Track the Expected Value of Contralateral Options.” *The Journal of Neuroscience: The Official Journal of the Society for Neuroscience* 29 (43): 13465–72.

Parker, Nathan F., Courtney M. Cameron, Joshua P. Taliaferro, Junuk Lee, Jung Yoon Choi, Thomas J. Davidson, Nathaniel D. Daw, and Ilana B. Witten. 2016. “Reward and Choice Encoding in Terminals of Midbrain Dopamine Neurons Depends on Striatal Target.” *Nature Neuroscience* 19 (6): 845–54.

Parkinson, J. A., J. W. Dalley, R. N. Cardinal, A. Bamford, B. Fehnert, G. Lachenal, N. Rudarakanchana, K. M. Halkerston, T. W. Robbins, and B. J. Everitt. 2002. “Nucleus Accumbens Dopamine Depletion Impairs Both Acquisition and Performance of Appetitive Pavlovian Approach Behaviour: Implications for Mesoaccumbens Dopamine Function.” *Behavioural Brain Research* 137 (1): 149–63.

Reynolds, John N. J., B. I. Hyland, and J. R. Wickens. 2001. “A Cellular Mechanism of Reward-Related Learning.” *Nature* 413 (6851): 67–70.

Reynolds, John N. J., and Jeffery R. Wickens. 2002. “Dopamine-Dependent Plasticity of Corticostriatal Synapses.” *Neural Networks: The Official Journal of the International Neural Network Society* 15 (4-6): 507–21.

Roesch, Matthew R., Donna J. Calu, and Geoffrey Schoenbaum. 2007. “Dopamine Neurons Encode the Better Option in Rats Deciding between Differently Delayed or Sized Rewards.” *Nature Neuroscience* 10 (12): 1615–24.

Russell, Stuart, and Andrew L. Zimdars. 2003. “Q-Decomposition for Reinforcement Learning Agents.” In *Proceedings of the Twentieth International Conference on International Conference on Machine Learning*, 656–63. ICML’03. Washington, DC, USA: AAAI Press.

Samuelson, P. A. 1938. “A Note on the Pure Theory of Consumer’s Behaviour.” *Economica* 5 (17): 61–71.

Saunders, Benjamin T., Jocelyn M. Richard, Elyssa B. Margolis, and Patricia H. Janak. 2018. “Dopamine Neurons Create Pavlovian Conditioned Stimuli with Circuit-Defined Motivational Properties.” *Nature Neuroscience* 21 (8): 1072–83.

Schultz, W., P. Dayan, and P. R. Montague. 1997. “A Neural Substrate of Prediction and Reward.” *Science* 275 (5306): 1593–99.

Silva, Joaquim Alves da, Fatuel Tecuapetla, Vitor Paixão, and Rui M. Costa. 2018. “Dopamine Neuron Activity before Action Initiation Gates and Invigorates Future Movements.” *Nature* 554 (7691): 244–48.

Soares, Sofia, Bassam V. Atallah, and Joseph J. Paton. 2016. “Midbrain Dopamine Neurons Control Judgment of Time.” *Science* 354 (6317): 1273–77.

Stan Development Team. 2018. PyStan: the Python interface to Stan, Version 2.17.1.0. http://mc-stan.org

Steinberg, Elizabeth E., Ronald Keiflin, Josiah R. Boivin, Ilana B. Witten, Karl Deisseroth, and Patricia H. Janak. 2013. “A Causal Link between Prediction Errors, Dopamine Neurons and Learning.” *Nature Neuroscience* 16 (7): 966–73.

Syed, Emilie C. J., Laura L. Grima, Peter J. Magill, Rafal Bogacz, Peter Brown, and Mark E. Walton. 2016. “Action Initiation Shapes Mesolimbic Dopamine Encoding of Future Rewards.” *Nature Neuroscience* 19 (1): 34–36.

Takahashi, Yuji, Geoffrey Schoenbaum, and Yael Niv. 2008. “Silencing the Critics: Understanding the Effects of Cocaine Sensitization on Dorsolateral and Ventral Striatum in the Context of an Actor/critic Model.” *Frontiers in Neuroscience* 2 (1): 86–99.

Ungerstedt, U., and G. W. Arbuthnott. 1970. “Quantitative Recording of Rotational Behavior in Rats after 6-Hydroxy-Dopamine Lesions of the Nigrostriatal Dopamine System.” *Brain Research* 24 (3): 485–93.

Ungless, Mark A., Peter J. Magill, and J. Paul Bolam. 2004. “Uniform Inhibition of Dopamine Neurons in the Ventral Tegmental Area by Aversive Stimuli.” *Science* 303 (5666): 2040–42.

Wise, Roy A. 2004. “Dopamine, Learning and Motivation.” *Nature Reviews. Neuroscience* 5 (6): 483–94.

Yin, Henry H., Barbara J. Knowlton, and Bernard W. Balleine. 2004. “Lesions of Dorsolateral Striatum Preserve Outcome Expectancy but Disrupt Habit Formation in Instrumental Learning.” *The European Journal of Neuroscience* 19 (1): 181–89.

Yttri, Eric A., and Joshua T. Dudman. 2016. “Opponent and Bidirectional Control of Movement Velocity in the Basal Ganglia.” *Nature* 533 (7603): 402–6.